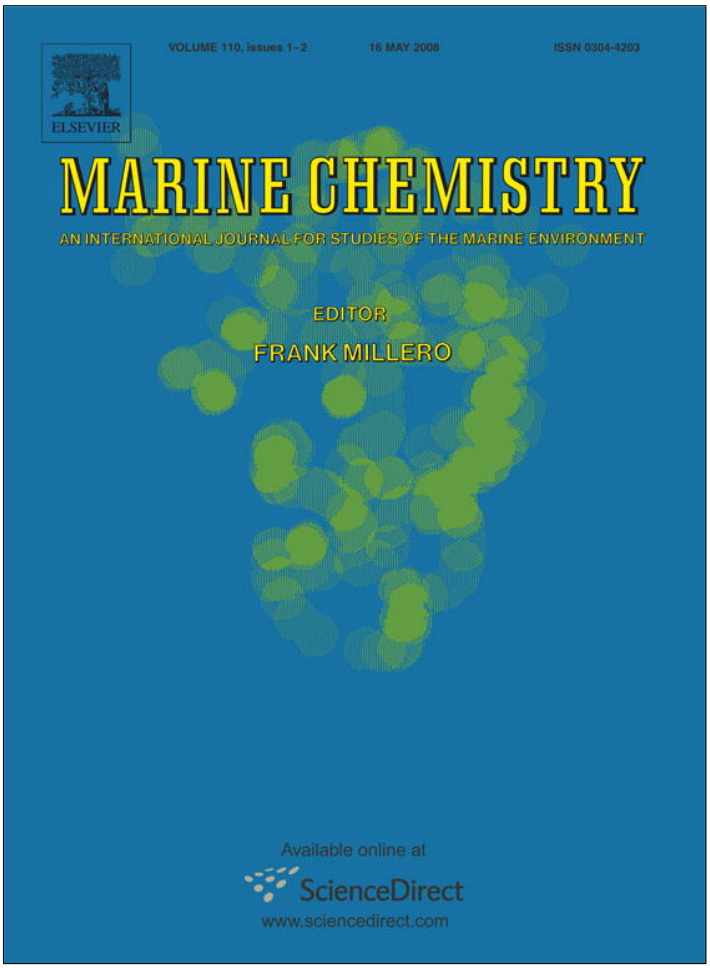

Marine Chemistry 110 (2008) 120–127

Contents lists available at ScienceDirect

Marine Chemistry

journal homepage: www.elsevier.com/locate/marchem

Geochemical and physical sources of radon variation in a subterranean estuary — Implications for groundwater radon activities in submarine groundwater discharge studies

H. Dulaiova *, M.E. Gonneea, P.B. Henderson, M.A. Charette

Woods Hole Oceanographic Institution, Department of Marine Chemistry and Geochemistry, Woods Hole, MA 02543, United States

ARTICLE INFO

Article history:
Received 30 September 2007
Received in revised form
21 December 2007
Available online 8 March 2008

Keywords:
Subterranean estuary
Geochemical tracers
Radon
Radium
Manganese
Groundwater
Submarine groundwater discharge
Geochemical transformations

ABSTRACT

Submarine groundwater discharge (SGD), from springs and diffuse seepage, has long been recognized as a source of chemical constituents to the coastal ocean. Because groundwater is two to four orders of magnitude enriched in radon compared to surface water, it has been used as both a qualitative and a quantitative tracer of groundwater discharge. Besides this large activity gradient, the other advantage of radon stems from its classification as noble gas; that is, its chemical behavior is expected not to be influenced by salinity, redox, and diagenetic conditions present in aquatic environments.

During our three-year monthly sampling of the subterranean estuary (STE) in Waquoit Bay, MA, we found highly variable radon activities (50–1600 dpm L^{-1}) across the fresh–saline interface of the aquifer. We monitored pore water chemistry and radon activity at 8 fixed depths spanning from 2 to 5.6 m across the STE, and found seasonal fluctuations in activity at depths where elevated radon was observed. We postulate that most of the pore water ^{222}Rn is produced from particle-surface-bound ^{226}Ra, and that the accumulation of this radium is likely regulated by the presence of manganese (hydr)oxides. Layers of manganese (hydr)oxides form at the salinity transition zone (STZ), where water with high salinity, high manganese, and low redox potential mixes with fresh water. Responding to the seasonality of aquifer recharge, the location of the STZ and the layers with radium enriched manganese (hydr)oxide follows the seasonal land- or bayward movement of the freshwater lens. This results in seasonal changes in the depth where elevated radon activities are observed.

The conclusion of our study is that the freshwater part of the STE has a radon signature that is completely different from the STZ or recirculated sea water. Therefore, the radon activity in SGD will depend on the ratio of fresh and recirculated seawater in the discharging groundwater.

1. Introduction and study site

Submarine groundwater discharge (SGD) facilitates transport of dissolved components from coastal aquifers to the sea (Valiela et al., 1990; Moore, 1996; Burnett et al., 2001; Slomp and van Cappellen, 2004). Groundwater advection rates to surface waters are often difficult to quantify but can be assessed indirectly via geochemical tracers such as radium isotopes and radon (Moore, 1996, 2000; Charette et al., 2001; Krest and Harvey, 2003; Burnett et al., 1996; Cable et al., 1996; Burnett and Dulaiova, 2003; McCoy et al., 2007; Martin et al., 2007). Radon has greater utility than radium as an SGD tracer where the discharge is fresh or a mixture of fresh and recirculated seawater since any groundwater in the aquifer (independent of its salinity) that is in contact with sediments and rocks is enriched in radon. This radon-enriched fluid is transported to coastal waters and a radon mass balance can be used to calculate total submarine groundwater discharge (e.g., Burnett and Dulaiova, 2003).

The major sources of uncertainty in the radon mass balance model are associated with (1) quantifying radon loss by evasion to the atmosphere (Dulaiova and Burnett, 2006), (2) quantifying radon loss via mixing with offshore waters

* Corresponding author. Tel.: +1 508 289 3739.
E-mail address: hdulaiova@whoi.edu (H. Dulaiova).

0304-4203/$ – see front matter © 2008 Elsevier B.V. All rights reserved.
doi:10.1016/j.marchem.2008.02.011

(Dulaiova et al., 2006a) and (3) characterizing the groundwater end-member radon activity that supplied the measured excess Rn in coastal waters (Christoff, 2001; Dulaiova et al., 2006b; Mulligan and Charette, 2006). Uncertainties associated with the latter are caused by natural heterogeneity of radon sources within one aquifer and/or the presence of multiple aquifers with different radon signatures discharging in the same area. Finding the true "representative" groundwater radon activity can be challenging but estimates are usually based on well, piezometer, and benthic flux chamber samples, or via a sediment radon equilibration method (Corbett et al., 1998).

This manuscript describes pore water radon (^{222}Rn) activities observed in a subterranean estuary (STE) in Waquiot Bay, MA (Fig. 1), where previous studies of groundwater composition have reported ^{222}Rn levels of 100–6000 dpm L^{-1}, depending on the season and depth sampled (Abraham et al., 2003; Mulligan and Charette, 2006). Since radon is an inert gas, we may expect its activity to be controlled mostly by sediment or rock uranium/radium content (which are the radioactive parents of Rn), and not by chemical reactions or pore water chemistry. However, ^{222}Rn ($t_{1/2}$ = 3.8 d) is produced via the radioactive decay of ^{226}Ra ($t_{1/2}$ = 1600 y), the chemistry of which is influenced by chemical and physical processes occurring in the aquifer (Moore, 1999). In general, anoxic groundwater is typically enriched in radium due to the mobilization of redox sensitive scavengers, in oxic waters radium strongly binds to manganese and, to a lesser extent, iron (hydr)oxides (Gonneea et al., in press).

The sedimentary deposits at the head of Waquoit Bay consist of outwash gravel, sand and silt (Oldale, 1976). The upper 10 m consists of homogeneous coarse-grained sand which is underlain by less permeable fine to very fine sand and silt. Sedimentology and pore water chemistry in the water-table aquifer has been described in detail by Charette and Sholkovitz (2002, 2006) and Charette et al. (2005). In those studies, sediment cores collected at the head of Waquoit Bay down to 2 m showed that the sediments contain 95% coarse sand and less than 5% silt and clays. The majority of the monomineralic grains are quartz and the polymineralic fragments are granite, schist, amphibolite and gabbro. The cores also contained traces of plagioclase, clinopyroxene, amphibole, white mica, magnetite and at least one other oxide (goethite or hematite). The color of the sand in the cores changed from tan to dark red, yellow and orange at the deeper layers. These layers had iron (hydr)oxide precipitates loosely bound to sand grains (Charette and Sholkovitz, 2002).

Based on pore water sampled to 8 m, these authors found a well defined subterranean estuary where fresh groundwater and recirculated seawater meet; here, the salinity transition zone (STZ) is 1–2 m deep. Within the freshwater portion of the aquifer, reducing fresh groundwater delivers high concentrations of dissolved ferrous iron and reduced manganese to the subterranean estuary. As this water mixes with saline water in the STZ, a large fraction of the dissolved Fe and Mn is oxidized and precipitates on organic C-poor quartz sand prior to discharge. Within the STZ and below, seasonal, diagenetically-produced reducing conditions result in Mn and Fe (hydr) oxide dissolution which is accompanied by a release of other elements that have an affinity for these phases. Such spatial and temporal variability makes the subterranean estuary a rather complex and dynamic system. These findings led to a time-series study in which pore water was sampled monthly across the salinity transition zone during a three-year period to investigate the seasonal oscillation of the STZ and resulting changes in groundwater chemistry (Gonneea et al., 2006).

Here we discuss the geochemical and physical drivers of radon variation in the Waquoit Bay subterranean estuary. We

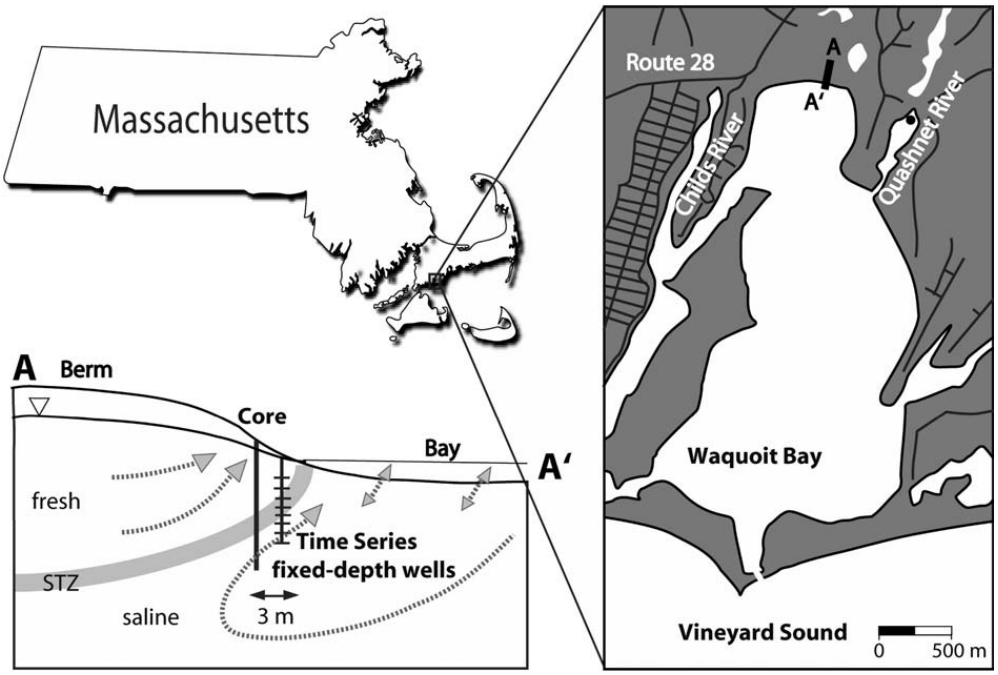

Fig. 1. Map of Waquoit Bay, MA with a schematic drawing of the subterranean estuary and our sampling locations. The sediment core and piezometer sampling in June 2006 took place at the site indicated on the schematics as "Core". STZ stands for the salinity transition zone in the aquifer where the groundwater salinity sharply increases from fresh to saline.

also discuss strategies for deriving a representative groundwater radon activity that is applicable for SGD studies at this site. Though the data presented here is limited to Waquoit Bay, MA, we expect that similar factors control radon activities in other STEs around the globe.

2. Methods

Groundwater samples were collected at the head of Waquoit Bay, MA at a location just above the mean sea level of the water line. In order to exclude variability in the STE due to tides, monthly sampling was always performed during the same phase of the tidal cycle (a few days before low spring tide) between the period of October 2004 and September 2007. A multi-level well constructed from nylon tubing and stainless-steel well points was set up at 8 discreet levels covering the full depth of the salinity transition zone at that site (2–6 m). Additional water samples were collected at 25 depths evenly distributed between 0.5 and 8 m at a location 3 m landward of the time-series well in June 2006. Water was sampled with a stainless-steel drive point piezometer (Charette and Allen, 2006) fitted with a clean nylon tube attached to a peristaltic pump. Salinity, dissolved oxygen, temperature, pH and ORP (standardized to Eh) were measured with a YSI 600XLM using a flow-through cell (YSI, Inc.). In addition, separate water samples were collected for salinity and analyzed with a Guideline AutoSal instrument. Duplicate samples for radon were collected in liquid scintillation vials pre-filled with 10 mL of mineral oil. Radon was analyzed on a Packard Tri-Carb 2750TR/LL low background scintillation counter (Prichard and Gessel, 1977). Some radon samples were collected into 250 mL bottles and analyzed with a Rad-H_2O system (Durride Inc.). These two radon analysis methods were cross-calibrated with excellent agreement between results. Four-liter groundwater samples were filtered through MnO_2 impregnated acrylic fibers at a flow rate of approximately 0.2 L/min to quantitatively sorb Ra onto the MnO_2 (Moore and Reid, 1973). The fibers were ashed, sealed with epoxy in gamma-vials, aged and counted by a well type gamma counter for ^{226}Ra via ^{214}Pb at 351.9 keV (Charette et al., 2001).

A 7-meter long sediment core was collected concurrently with water samples at the site of the piezometer deployment in June 2006. The sediment was collected with a hand-operated bailer boring auger which allowed a theoretical sampling resolution of 60 cm. The samples were bagged individually and stored at 4 °C until analysis. Subsamples of

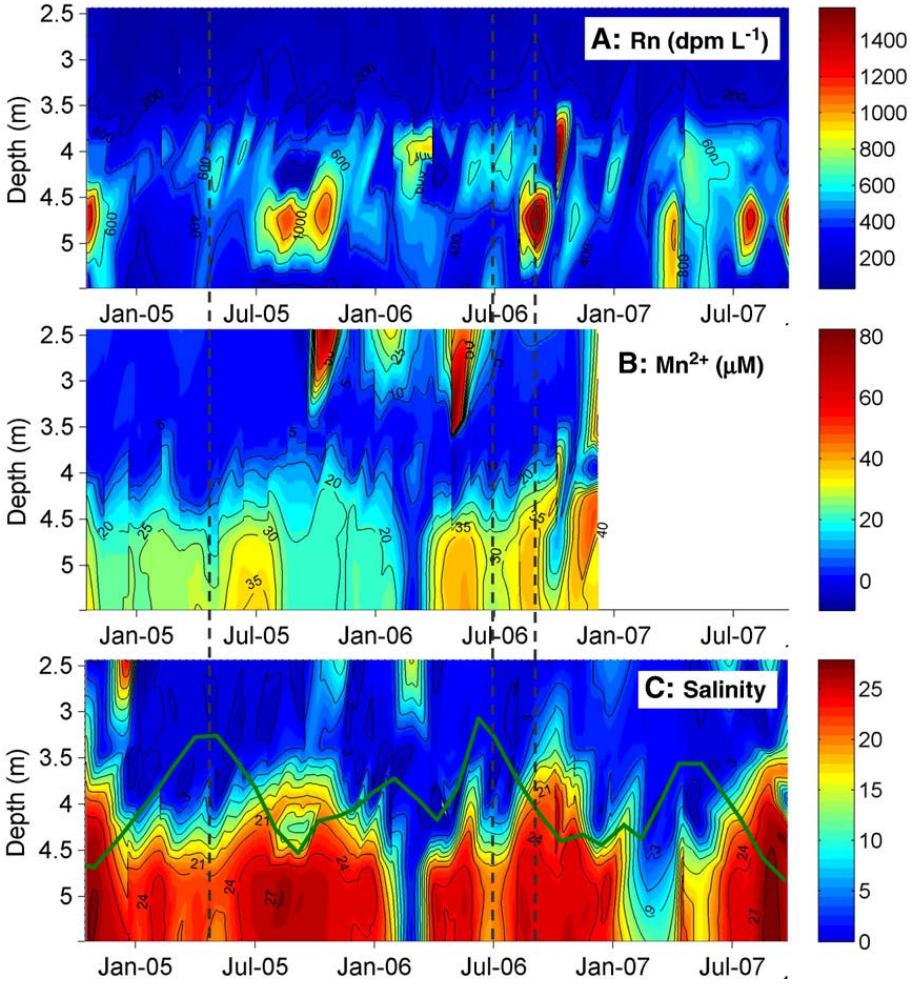

Fig. 2. Results from time-series measurements of pore water chemistry at fixed depths from 2.3 to 5.5 m of A. ^{222}Rn (dpm L^{-1}), B. dissolved Mn^{2+}, and C. salinity. The contour plots indicate the chemical property with high values in reds and low values in blue colors, the *x*-axis indicates time and the *y*-axis indicates depth below surface (m). Water level in a groundwater well located near Waquoit Bay, MA is overlain on the time-series salinity contours. The black dashed lines indicate time points plotted on Fig. 4. (For interpretation of the references to colour in this figure legend, the reader is referred to the web version of this article.)

the core were dried, sealed with epoxy, aged, and then counted on planar gamma detectors for bulk sediment ^{226}Ra via ^{214}Pb at 351.9 keV and ^{238}U via ^{234}Th at 63 keV. A portion of each sediment sample was subjected to an operationally defined leach to determine the concentrations of Fe, Mn, Th, Ba, and U associated with amorphous and crystalline oxides of Fe and Mn (Hall et al., 1996). The samples were analyzed on a Finnigan Element high resolution ICP-MS at Woods Hole Oceanographic Institution (Gonneea et al., in press).

To measure sediment equilibrium radon activities, ~100 g of wet mixed sediment from depth intervals of 2.1 to 3 m, 4.6 to 5.5 m, and 5.8 to 6.5 m were mixed with 0.5 L Ra-free Waquoit Bay groundwater with salinity 11 in 1 L HDPE bottles. The bottles were capped airtight with lids fitted with tubing for helium circulation during analysis (Stringer and Burnett, 2004). The samples were kept sealed for >20 days prior to analysis and then the radon was flushed into a cold trap and scintillation cells using helium, and finally counted on alpha scintillation counters (Corbett et al., 1998). Each sample was prepared in duplicate and analyzed three times. The measured radon activities in dpm g^{-1} wet sediment were converted to pore water radon activities (dpm L^{-1}) assuming a wet bulk density of 1.9 g cm^{-3} and porosity of 0.4.

3. Results

The time-series groundwater salinity profiles plotted in Fig. 2C show strong seasonality at almost all depths. In the usually fresh (salinity 0–1) top layer, salinity increases to 10–20 in some fall and winter months perhaps due to overtopping of seawater during storm events. The salinity gradient is the steepest between 3.5 and 4.5 m within which salinity ranges from 1 to 25. This region shows seasonal fluctuations, with low salinity in the spring and high salinity in the summer and fall. The same trend is evident in the deeper sediments below 4.5 m where salinity fluctuates in a narrower range, between 20 and 25. The freshening events in the middle and lower layers are well correlated with periods of elevated groundwater level at a nearby monitoring well (USGS site #413525070291904, Mashpee, MA). This correlation clearly indicates vertical and horizontal expansions of the freshwater lens as the aquifer recharges in winter and spring.

Radon activities measured in the multi-level well over the two-year period from October 2004 to September 2007 varied between 50 and 1600 dpm L^{-1} (Fig. 2A). We measured low activities in the top 2.4 to 3.5 m with values ranging from 50 to 200 dpm L^{-1} (average 113±30 dpm L^{-1}). The largest variability occurred between 3.5 and 5 m with activities from 200 to 1600 dpm L^{-1}. Samples collected below 5.5 m had a smaller seasonal fluctuation, with radon ranging from 150 to 550 dpm L^{-1}. The highest levels of radon were measured at 4.7 m during the summer and fall and at 4 m in the spring and early summer (Fig. 2A).

Radon measured in groundwater at a location 3 m landward of the time-series well in June 2006 also showed variability with depth (Fig. 3A). The activities were constant (average 120±40 dpm L^{-1}) down to 4.5 m then increased to a double peak at 5.5 (1200 dpm L^{-1}) and 6.1 m (2300 dpm L^{-1}). The values below 6.1 m decreased to <400 dpm L^{-1}.

Dissolved pore water ^{226}Ra activities were low in the fresh surface layer (average 0.11±0.09 dpm L^{-1}). High seasonal radium fluctuation occurred at 2.7 to 4.5 m with maximum

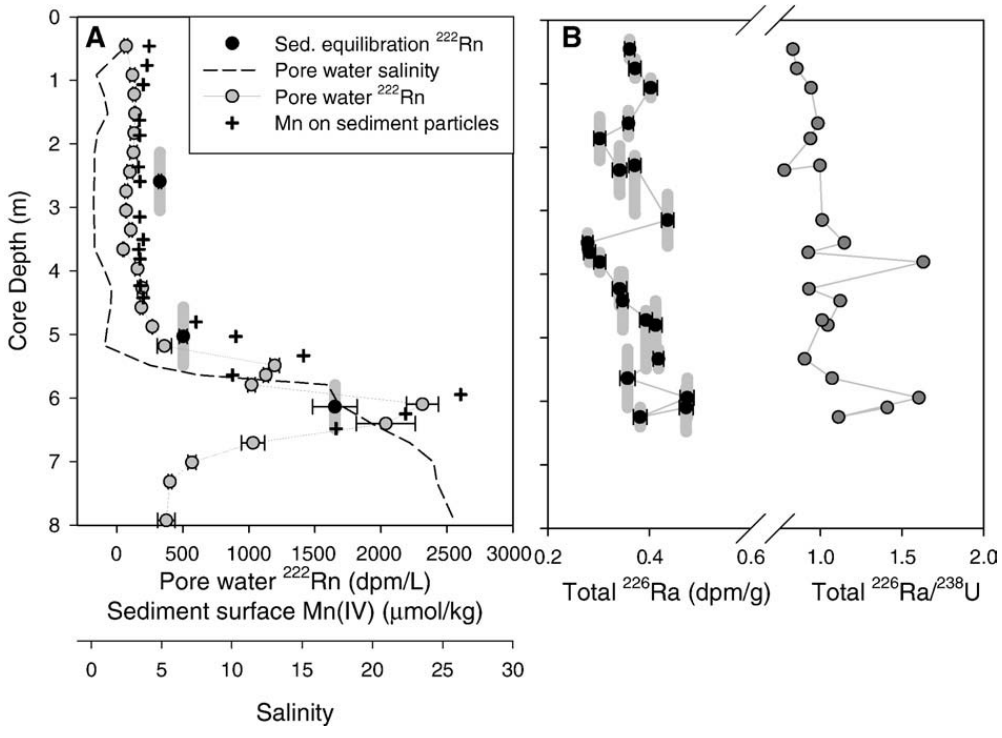

Fig. 3. A. Pore water salinity (dashed line) and ^{222}Rn (grey circles, dpm L^{-1}), sediment bound Mn (crosses, µmol kg^{-1}) and sediment equilibrium ^{222}Rn (black circles, dpm L^{-1}) measured in June 2006 plotted against depth (m). The vertical uncertainty bars on the sediment equilibrium ^{222}Rn values represent the depth range of sediments mixed together for each sample. B. Total bulk sediment ^{226}Ra (dpm g^{-1}) and ^{226}Ra/^{238}U ratios measured by gamma-spectrometry. The vertical uncertainty bars on the bulk ^{226}Ra values represent the depth range of sediments mixed together for each sample.

^{226}Ra of up to 15 dpm L^{-1} in the fall months. Below 4.5 m the dissolved radium levels were steady at an average of 0.45±0.15 dpm L^{-1}. Bulk sediment ^{226}Ra activities ranged from 0.28 dpm g^{-1} at the top of the core to 0.49 dpm g^{-1} at 6.1 m. The calculated ^{226}Ra/^{238}U ratios measured by gamma-spectrometry were 0.8 to 1.9.

Pore water equilibrium radon measured by the sediment equilibration experiment was 226±7 dpm L^{-1} in sediments collected from 2.1 to 3 m (average depth 2.6 m), 350±20 dpm L^{-1} at 4.6 to 5.5 m (average 5 m), and 1150±120 dpm L^{-1} at 5.8 to 6.5 m (average 6.1 m). These equilibrium radon activities can also be used as an estimate of surface-bound ^{226}Ra, which are 0.075±0.002 dpm g^{-1} (20% of bulk ^{226}Ra), 0.114±0.007 dpm g^{-1} (29% of bulk ^{226}Ra), and 0.38±0.04 dpm g^{-1} (76% of bulk ^{226}Ra), respectively.

There is a strong positive correlation of dissolved manganese and salinity (Fig. 2B) with high concentrations (~40 µmol L^{-1}) occurring at the highest salinities (26). We also found a good correlation between pore water dissolved and solid-phase manganese in the sediments collected in June 2006. The solid state manganese in this core was determined from sediment leaching experiments designed to reduce the amorphous and crystalline Fe and Mn (hydr)oxides. The adsorbed sedimentary Mn concentration spanned from 40 µmol kg^{-1} on the top to 2500 µmol kg^{-1} near the bottom of the core (Fig. 3).

4. Discussion

4.1. The mechanism of radon enrichment in the STE and the sources of its variability

The sole source of ^{222}Rn ($t_{1/2}$=3.8 d) in groundwater is the radioactive decay of ^{226}Ra ($t_{1/2}$=1600 y), where 50% of the equilibrium radon activity builds up in 3.8 days and 98% is reached within 21 days. Radium, the parent of radon, can be bound in the mineral lattice in aquifer solids, retained on grain surface coatings, and dissolved in pore water. The former two fractions are collectively referred to as the labile ^{226}Ra pool. The fraction of radon produced from lattice bound radium and ejected or leached into the water after alpha-recoil is very low (10^{-5}; Tricca et al., 2001). The two remaining radon sources are: (1) production from radium retained in surface coatings followed by ejection or diffusion into the water, and (2) ingrowth from radium dissolved in pore water.

Sources of this labile ^{226}Ra pool in the vadose zone include recoil, weathering, and advective transport of radium from upstream locations in the aquifer. Based on chemical and physical conditions in the aquifer, which will be discussed in the following paragraphs, this radium is distributed as surface bound or dissolved. At our sampling site, dissolved radium activity varies a great deal with depth; for example, we recorded elevated levels at 2.7 to 4.5 m. However, this radium cannot account for the observed radon variability, because radon activities produced by the decay of dissolved radium are orders of magnitude lower than the observed pore water radon values. Even the highest measured pore water ^{226}Ra (15 dpm L^{-1}) could only support 1–10% of the observed radon. Therefore we surmise that the observed increases in radon activities in the pore water must be produced mostly by the decay of surface-bound radium within the STE. Groundwater advection rates calculated using Darcy's law were 0.09–0.43 m d^{-1} within this part of the aquifer (Mulligan and Charette, 2006). This flow is fast enough to transport long-lived isotopes such as ^{226}Ra ($t_{1/2}$=1600 y) for significant distances; for example, from upland locations in the aquifer to coastal sediments. However at these flow rates and assuming homogeneous radium distribution along groundwater flow paths, ^{222}Rn ($t_{1/2}$=3.8 d) activities would be re-established as often as every 2 to 10 m reflecting radon production rates along groundwater flow lines. We observed that radon activities measured in pore water in June 2006 agreed very well with those obtained by sediment equilibration experiments (Fig. 3). If radon was produced locally, the two results should be comparable (compared to in situ conditions, radon activities attained from the sediment equilibration technique are usually about 10% higher due to the slurrying process (Berelson et al., 1982)). This supports the fact that radon in the pore water must be produced locally from the decay of radium retained in the surface coating of particles in the immediate vicinity of the pore water sampling point. Seasonal radon variations must then be explained by the labile radium accumulation and release in the STE.

In the following we describe a possible mechanism of seasonal variation of surface-bound radium activities in the sediments of the STE. In Waquoit Bay, the position of the salinity transition zone changes seasonally as the size of the freshwater lens responds to changing precipitation (Michael et al., 2005). During the winter and spring recharge period, freshwater flow increases and the STZ moves seaward. During the summer and fall, aquifer levels decline, and the STZ moves landward, inundating more sediments with saline water. The shifts in the regions of fresh/saline and reducing/less reducing environments are demonstrated in the time-series salinity profiles and groundwater levels observed in a nearby monitoring well (Fig. 2C). Gonneea et al. (in press) found that in the STZ Ra is sorbed onto Fe and Mn (hydr)oxides precipitating at the interface between the buffered saline water (high pH, low $p\varepsilon$ and high dissolved Mn and Fe concentrations) and fresh shallow groundwater (relatively low pH and high $p\varepsilon$). Although Ra has higher affinity for Mn (hydr)oxides (Moore and Reid, 1973), Fe (hydr)oxides occur in one order of magnitude higher concentrations and may have just as much influence on the aquifer Ra distribution. As described in the following paragraphs, we observed very good correlation between pore water radon collected in June 2006 and solid-phase manganese in the core but not iron. Although we cannot rule out the possibility that radon is more closely correlated with iron (hydr)oxides during the winter months or in deep sediments, we will mostly focus on its relation with manganese.

Radium is associated with Fe and Mn (hydr)oxides either by non-selective co-precipitation during their formation or with a chemical bond which is different from the physical Ra sorption onto particulates in low ionic-strength environments. In the absence of Fe and Mn (hydr)oxides in sediments, Ra can quickly desorb as the salinity of the pore water increases (Elsinger and Moore, 1980). When radium is bound to Fe and Mn (hydr)oxides, the potential release under reducing conditions is much greater than desorption driven only by increases in ionic strength (Gonneea et al., in press).

The dissolved manganese pool is associated with the high salinity region of the STE, which also contains elevated

dissolved Ra (Gonneea et al., in press; Charette and Sholkovitz, 2006). Because we sampled at fixed horizons, this pool of water was captured in our time-series observations only in the summer months, when the freshwater lens receded and the STZ moved to shallower depths (<4 m), as indicated by the decreasing groundwater level in the monitoring well (Fig. 2C). Elevated salinity, pH, and dissolved Mn appeared at 4.5–5.5 m in Jun 2005, Apr 2006, Aug 2006, and June 2007. Although salinity was elevated for several months, dissolved Mn concentrations decreased over time in the same period. We calculated that, under the observed pH and $p\varepsilon$ ranges in the STZ, the Mn species equilibrium state often favors the formation of solid state MnOOH and $Mn(OH)_2$ (Stumm and Morgan, 1996). For each solid Mn (hydr)oxide species, we derived the theoretical ratio of solid to dissolved manganese $\{Mn^{2+}\}$ for given pH and $p\varepsilon$ values. For example, for MnOOH:

$$\log \frac{\{\gamma - \mathrm{MnOOH(s)}\}}{\{Mn^{2+}\}} = -25.3 + 3\mathrm{pH} + p\varepsilon. \quad (1)$$

Where a higher ratio implies that γ-MnOOH precipitation is thermodynamically more favorable. Fig. 4 shows pore water properties for three selected times: May 2005 (wet period, high groundwater level) and September 2006 (dry period, low groundwater level) in the permanent wells. The July 2006 (wet period) profile sampled to 8 m is also shown. In addition, the potential for solid Mn species formation is displayed. It is calculated based on the observed pH and $p\varepsilon$ values (Eq. (1)). During May 2005, groundwater level was high and the freshwater lens expanded bayward. The highest observed salinity at 5.6 m was ~20, pore water Mn across the profile was low, and the potential to form MnOOH was also low. The highest observed radon was 600 dpm L^{-1}. On the other hand, in the dry period in September 2006, we measured salinities >25 and the formation potential of solid Mn species in the deeper layers was high ($\{\gamma\text{-}MnOOH_{(s)}\}/\{Mn^{2+}\} > 10^3$). At these layers radon activities reached 1600 dpm L^{-1}. Based on these results we conclude that under favorable pH, $p\varepsilon$ and Mn^{2+} concentrations, Mn (hydr)oxides precipitate and sorb Ra. Radium is also continuously supplied by lateral groundwater flow. This enrichment in surface-bound radium leads to the observed elevated pore water radon activities. The above-described process of Ra accumulation is supported by the fact that elevated radon activities at 5 m coincide with low groundwater levels. Radon increases coinciding with water level decline is most pronounced in October 2004, September 2005, September 2006, and September 2007 (Fig. 2A and C).

The results from the sediment core analysis further support the above-described theory. The location of the June 2006 sampling site is 3 m landward of the time-series well, where the STZ lies about 1 m deeper. We found a remarkable correlation between pore water radon activities and particulate Mn concentrations (Fig. 3A). The double peak in the concentration of these elements at 5.5 and 6.1 m appears on both profiles. In the absence of sufficient dissolved ^{226}Ra, the source of elevated ^{222}Rn must be ^{226}Ra adsorbed on the Mn (hydr)oxide coating of sand grains. Although bulk ^{226}Ra measured by gamma-spectrometry does not reveal a pronounced increase in total radium with depth, the ratio of total- to lattice-bound radium approximated by a ratio of $^{226}Ra/^{238}U$ peaks at 6.1 m, exactly where the Mn and Rn maximums are. Moreover, the sediment equilibration experiments resulted in the same radon values observed in the pore

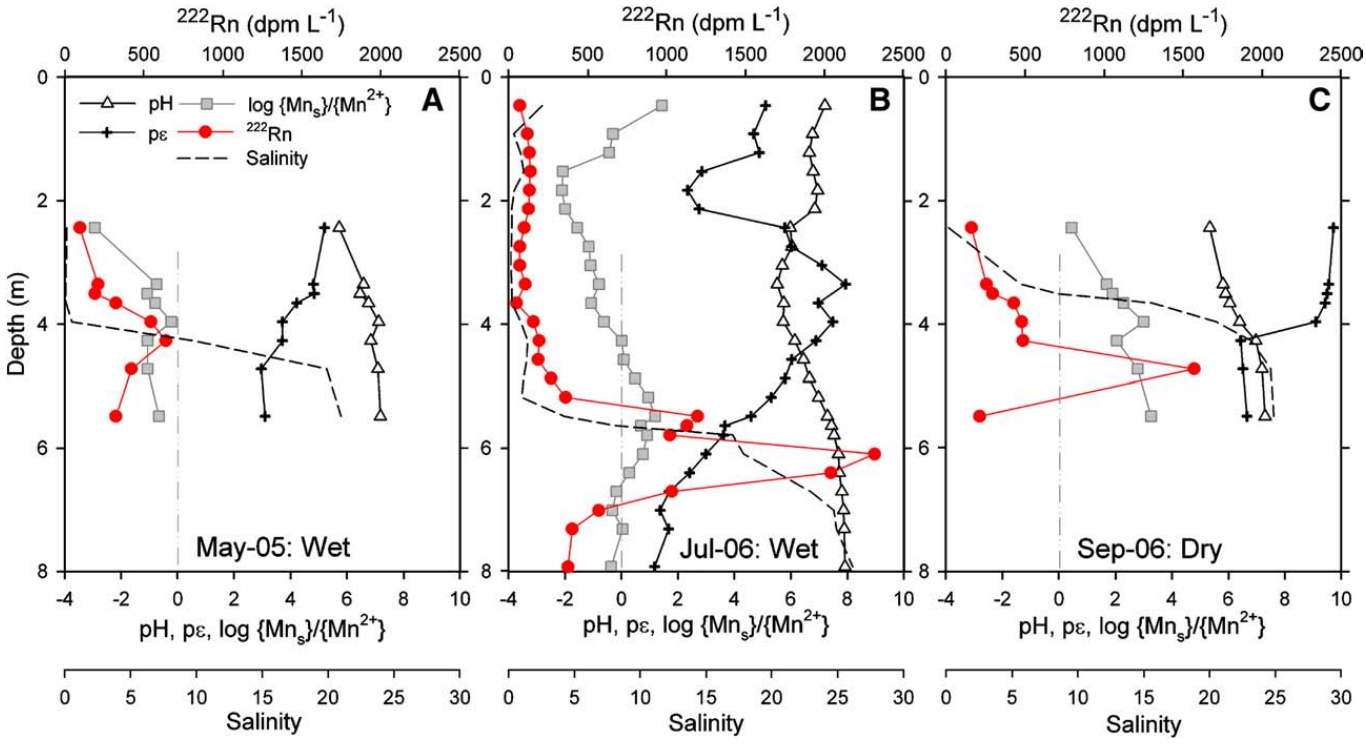

Fig. 4. Pore water properties A. in permanent wells in May 2005 during high groundwater level representing a wet period (see also Fig. 2C), B. July 2006 profile sampled to 8 m (also during a wet period), and C. in permanent wells in September 2006 during falling/low groundwater level. For all dates, also shown is the potential for solid Mn species formation calculated based on the observed pH and $p\varepsilon$ values (Eq. (1)). From the comparison of figures A and C with B, it is obvious that the permanent wells only monitor a limited section of the subterranean estuary.

water samples. This provides evidence that there is enough surface-bound radium to produce the observed radon profiles.

We conclude that in the dynamic environment of the STE, pore water radon activities are regulated by the following simplified relationship:

$$\uparrow p\varepsilon,\ \uparrow \mathrm{pH},\ \uparrow \mathrm{Mn}^{2+} \rightarrow \ll \frac{\{\mathrm{Mn_s}\}}{\{\mathrm{Mn_{dis}}\}} \rightarrow \mathrm{Mn_s} - {}^{226}\mathrm{Ra} \rightarrow {}^{222}\mathrm{Rn},$$

Based on Eq. (1), high $p\varepsilon$, pH and dissolved Mn^{2+} facilitate the formation of solid Mn (hydr)oxides. These precipitates then accumulate radium, which in turn supports the ingrowth of high pore water radon. Conversely, lower $p\varepsilon$ and pH lead to the dissolution of Mn (hydr)oxides, and lower pore water radon concentrations as radium is released and transported away by groundwater flow.

4.2. Consequences of groundwater radon variability for SGD studies

Our results show that one must carefully consider sampling locations for radon in wells and piezometers. Sites chosen based on accessibility or sampling tool availability may not provide the most representative radon activity. Commonly, an average or median value of several measurements is used to derive the best groundwater radon estimates for submarine groundwater discharge studies (Dulaiova et al., 2006; Abraham et al. 2003).

The most appropriate method for deriving a properly weighed average end-member activity is by sampling across the full salinity gradient to capture the full extent of radon variability. Once the representative radon activity is known for each water type contributing to SGD (usually divided into fresh groundwater and recirculated seawater components), the representative radon activity can be estimated based on the ratio of the magnitudes of these components. For Waquoit Bay, the ratio of fresh and salt water discharge in SGD has been described by Michael et al. (2005) and Mulligan and Charette (2006). Fresh water outflow from the aquifer occurs at a nearly constant rate year-round, in some simulations with slightly higher discharge rates in late spring and summer. This flow represents at least 50% of the total SGD in the spring and summer, and 75–90% in the fall and winter. The remaining fraction of SGD occurs in the form of recirculated seawater, due to tidal pumping and dispersive circulation. This flow takes place on the bayward edge of the STZ. Intense salt water outflow occurs in late spring and summer during peak fresh water discharge.

Radon measured in the fresher part of the aquifer (0.5 to 3.5 m) during the time-series sampling was 120±40 dpm L^{-1} year-round. Radon activities in the salinity transition zone with brackish water can be as high as 2000 to 6000 dpm L^{-1}. In the saline part of the STE (in the permanent well captured in the fall and winter) radon activities are more uniform (410±190 dpm L^{-1}). Therefore, 400 dpm L^{-1} is an appropriate groundwater radon activity for recirculated seawater. Assuming fresh to salty groundwater discharge ratios of 1:1 in the summer and 9:1 in the winter, we expect the effective groundwater end-member radon activity to range from 320 dpm L^{-1} in the spring and summer to 148 dpm L^{-1} in the fall and winter. These calculations, however, do not assume any radon contribution from the brackish zone, in which radon values are disproportionately higher (>1500 dpm L^{-1}). Whether such high activities in the aquifer discharge to the surface will depend on two conditions: (1) Does the trend of high Mn (hydr)oxides with abundant surface-bound radium continue all the way to the bay? (2) Even if the trend does not extend to the bay, does it reach far enough so that high radon can be transported by groundwater flow to the surface? The scenario of the high Mn (hydr)oxide-radon trend described in case (1) is possible if the redox boundaries fall along the salinity gradient, and the groundwater flow is along the isopycnals. In addition, it is likely that redox conditions in either the intermediate organic rich layer or oxygenated surface sediments at the seepage face disrupt the optimal pH and $p\varepsilon$ pattern that allows the formation of Mn (hydr)oxides. Should this disruption occur within a few meters of the point of surface discharge, high radon will still be transported by groundwater flow to the bay. As we described earlier, radon in this part of the aquifer can propagate by groundwater flow as far as 2–10 m.

Charette et al. (2005) sampled a cross-section of this STE and showed that the salinity trends and dissolved manganese pool indeed extend all the way to the bay resulting in high probability for the elevated Rn activities to reach the surface. Again, based on Michael et al. (2005) the discharge of saline groundwater at the Waquoit Bay study site is only significant in the summer months. Depending on the sampling and SGD conditions, one may even limit radon sampling to the fresh- and brackish water part of the STE in the winter when none or very little recirculated seawater discharge is expected.

Ultimately, it is important to note that radon activities measured several meters inland from the site of groundwater discharge may only be relevant if the sediments are homogeneous along the flow path. Otherwise, pore water sampling at the point of discharge or sediment equilibration experiments with sediments collected at the point of discharge may provide a more accurate effective groundwater end-member radon activities. In either of the two cases mentioned above, spatial heterogeneity must be considered when choosing sites for sediment and pore water sample collection.

5. Conclusions

Complex redox and mixing processes in the subterranean estuary influence the distributions of Mn and ^{226}Ra between sediment particle surfaces and pore water. We postulate that radium accumulation on Mn (hydr)oxides ultimately drives ^{222}Rn pore water activities. Seasonal monitoring of the STE or sampling across the full salinity gradient, may be necessary to derive the best representative groundwater end-member radon activities. In designing a groundwater radon sampling strategy for a subterranean estuary, one must allow for (1) heterogeneity in pore water chemistry with depth and distance from the shoreline; (2) variable sediment surface chemistry; and (3) large seasonal variability in the composition of discharging groundwater, especially in regions most influenced by redox or salinity changes.

Acknowledgements

The authors thank Gillian Smith, Paul J. Morris, and DeAnna McCadney for assistance in the field and laboratory. David Schneider of the WHOI ICP-MS Facility performed the trace metal analyses. We thank Billy Moore, Alex Rao, and two anonymous reviewers for their constructive comments on the manuscript. We extend our continued appreciation to the director and staff of the Waquoit Bay National Estuarine Research Reserve for their assistance with logistics during field sampling. This work is a result of research sponsored by NSF (OCE-0425061 to M.A.C.) and the WHOI Postdoctoral Scholar program (to H.D.).

References

Abraham, D.M., Charette, M.A., Allen, M.C., Rago, A., Kroeger, K.D., 2003. Radiochemical estimates of submarine groundwater discharge to Waquoit Bay, Massachusetts. Biol. Bull. 205, 246–247.

Berelson, W.M., Hammond, D.E., Fuller, C., 1982. Radon-222 as a tracer for mixing in the water column and benthic exchange in the southern California borderland. Earth Planet. Sci. Lett. 61, 41–54.

Burnett, W.C., Taniguchi, M., Oberdorfer, J., 2001. Measurement and significance of the direct discharge of groundwater into the coastal zone. J. Sea Res. 46 (2), 109–116.

Burnett, W.C., Cable, J.E., Corbett, D.R., Chanton, J.P., 1996. Tracing groundwater flow into surface waters using natural ^{222}Rn. 1996 In: Buddemeier, R.W. (Ed.), Groundwater Discharge in the Coastal Zone: Proceedings of an International SymposiumLOICZ Reports and Studies, vol. 8. LOICZ, Texel, The Netherlands, pp. 22–28.

Burnett, W.C., Dulaiova, H., 2003. Estimating the dynamics of groundwater input into the coastal zone via continuous radon-222 measurements. J. Environ. Radioact. 69, 21–35.

Cable, J.E., Burnett, W.C., Chanton, J.P., Weatherly, G.L., 1996. Estimating groundwater discharge into the northeastern Gulf of Mexico using radon-222. Earth Planet. Sci. Lett. 144, 591–604.

Charette, M.A., Buesseler, K.O., Andrews, J.E., 2001. Utility of radium isotopes for evaluating the input and transport of groundwater-derived nitrogen to a Cape Cod estuary. Limnol. Oceanogr. 46, 465–470.

Charette, M.A., Sholkovitz, E.R., 2002. Oxidative precipitation of groundwater-derived ferrous iron in the subterranean estuary of a coastal bay. Geophys. Res. Lett. 29 2001GL014512.

Charette, M.A., Sholkovitz, E.R., Hansel, C., 2005. Trace element cycling in a subterranean estuary: part 1. geochemistry of the permeable sediments. Geochim. Cosmochim. Acta 69, 2095–2109.

Charette, M.A., Sholkovitz, E.R., 2006. Trace element cycling in a subterranean estuary: part 2. geochemistry of the pore water. Geochim. Cosmochim. Acta 70, 811–826.

Charette, M.A., Allen, M.C., 2006. Precision ground water sampling in coastal aquifers using a direct-push, shielded-screen well-point system. Ground Water Monit. R. 26 (2), 87–93.

Christoff, J.L., 2001. Quantifying groundwater seepage into a shallow near-shore coastal zone by two techniques. M.S. Thesis, Florida State University, p.120.

Corbett, D.R., Burnett, W.C., Cable, P.H., Clark, S.B., 1998. A multiple approach to the determination of radon fluxes from sediments. J. Radioanal. Nucl. Chem. 236, 247–252.

Dulaiova, H., Burnett, W.C., 2006. Radon loss across the water–air interface (Gulf of Thailand) estimated experimentally from ^{222}Rn–^{224}Ra. Geophys. Res. Lett. 33, L05606. doi:10.1029/2005GL025023.

Dulaiova, H., Burnett, W.C., Chanton, J.P., Moore, W.S., Bokuniewicz, H.J., Charette, M.A., Sholkovitz, E., 2006a. Assessment of submarine groundwater discharges into West Neck Bay, New York, via natural tracers. Cont. Shelf Res. 26 (16), 1971–1983.

Dulaiova, H., Burnett, W.C., Wattayakorn, G., Sojisuporn, P., 2006b. are groundwater inputs into river-dominated areas important? The Chao Phraya River — Gulf of Thailand. Limnol. Oceanogr. 51 (5), 2232–2247.

Elsinger, R.J., Moore, W.S., 1980. ^{226}Ra behavior in the Pee Dee River–Winyah Bay Estuary. Earth Planet. Sc. Lett. 48, 239–249.

Gonneea, M.E., Mulligan, A., Charette, M.A., 2006. Seasonal trends in radium activities within the mixing zone of a subterranean estuary, Waquoit Bay, MA. Eos Transactions AGU Ocean Sciences Meeting Supplement, vol. 87(36). Abstract OS15B-01.

Gonneea, M.E., Morris, P.K., Dulaiova, H., Charette, M.A., in press. New perspectives on radium behavior within a subterranean estuary. Marine Chemistry.

Hall, G.E.M., Vaive, J.E., Beer, R., Hoashi, M., 1996. Selective leaches revisited, with emphasis on the amorphous Fe oxyhyxroxide phase extraction. J. Geochem. Explor. 56, 59–78.

Krest, J.M., Harvey, J.W., 2003. Using natural distributions of short-lived radium isotopes to quantify groundwater discharge and recharge. Limnol. Oceanogr. 48 (1), 290–298.

Martin, J.B., Cable, J.E., Smith, C., Roy, M., Cherrier, J., 2007. Magnitudes of submarine groundwater discharge from marine and terrestrial sources: Indian River lagoon, Florida. Water Reasour. Res. 43, W05440. doi:10.1029/2006WR005266.

McCoy, C.A., Corbett, D.R., Cable, J.E., Spruill, R.K., 2007. Hydrogeological characterization of southeast coastal plain aquifers and groundwater discharge to Onslow Bay, North Carolina (USA). J. Hydrol. 339, 159–171.

Michael, H.A., Mulligan, A.E., Harvey, C.F., 2005. Seasonal oscillations in water exchange between aquifers and the coastal ocean. Nature 436, 1145–1148.

Moore, W.S., Reid, D.F., 1973. Extraction of radium from natural waters using manganese-impregnated acrylic fibers. J. Geophys. Res. 90, 6983–6994.

Moore, W.S., 1996. Large groundwater inputs to coastal waters revealed by ^{226}Ra enrichments. Nature 380, 612–614.

Moore, W.S., 1999. The subterranean estuary: a reaction zone of ground water and sea water. Mar. Chem. 65, 111–125.

Moore, W.S., 2000. Determining coastal mixing rates using radium isotopes. Cont. Shelf Res. 20, 1993–2007.

Mulligan, A.E., Charette, M.A., 2006. Intercomparison of submarine groundwater discharge estimates from a sandy unconfined aquifer. J. Hydrol. 327, 411–425.

Oldale, R.N., 1976. Notes on the generalized geologic map of Cape Cod. U. S. Geological Survey Open-File Report, pp. 76–765.

Prichard, H.M., Gesell, T.F., 1977. Rapid measurements of ^{222}Rn concentrations in water with a commercial liquid scintillation counter. Health Phys. 33, 577–581.

Slomp, C.P., van Cappellan, P., 2004. Nutrient inputs to the coastal ocean through submarine groundwater discharge: controls and potential impact. J. Hydrol. 295, 64–86.

Stringer, C.E., Burnett, W.C., 2004. Sample bottle design improvements for radon emanation analysis of natural waters. Health Phys. 87, 642–646.

Stumm, W., Morgan, J.J., 1996. Aquatic chemistry: chemical equilibria and rates in natural waters, third ed. John Wiley&sons, Inc., p. 1022.

Tricca, A., Wasserburg, G.J., Porcell, D., Baskaran, M., 2001. The transport of U- and Th-series nuclides in a sandy unconfined aquifer. Geochim. Cosmochim. Acta 65, 1187–1210.

Valiela, I., Costa, J., Foreman, K., Teal, J.M., Howes, B., Aubrey, D., 1990. Transport of groundwater-borne nutrients from watersheds and their effects on coastal waters. Biogeochem. 10, 177–197.